SUPERCONDUCTIVITY IN DOPED FULLERENES

While there is not complete agreement on the microscopic mechanism of superconductivity in alkali-metal-doped C_{60}, further research may well lead to the production of analogous materials that lose resistance at even higher temperatures.

Arthur F. Hebard

Carbon 60 is a fascinating and arrestingly beautiful molecule. With 12 pentagonal and 20 hexagonal faces symmetrically arrayed in a soccer-ball-like structure that belongs to the icosahedral point group I_h, its high symmetry alone invites special attention.[1] The publication in September 1990 of a simple technique[2] for manufacturing and concentrating macroscopic amounts of this new form of carbon (see Donald R. Huffman's article in PHYSICS TODAY, November 1991, page 22) announced to the scientific community that enabling technology had arrived. Macroscopic amounts of C_{60} (and the higher fullerenes, such as C_{70} and C_{84}) can now be made with an apparatus as simple as an arc furnace powered with an arc welding supply. Accordingly, chemists, physicists and materials scientists have joined forces in an explosion of effort to explore the properties of this unusual molecular building block.

Through the early work on graphite intercalation compounds[3] the basic ideas that spearheaded rapid advances in understanding had already been put in place. At the simplest level, a C_{60} molecule can be thought of as a graphite sheet rolled into a sphere. Although pentagons replace some of the hexagons to induce curvature, the average carbon–carbon distance on the surface of the molecule remains essentially the same as the carbon–carbon distance (1.42 Å) between the threefold-coordinated intraplanar carbon atoms of graphite. C_{60} molecules form a spherically close-packed solid with a face-centered cubic structure. (See the left panel of figure 1.) The C_{60} spheres, separated from each other by 10 Å, are held together by van der Waals forces. The analogy between solid C_{60} and graphite intercalation becomes evident when one realizes that for fcc hard-sphere packing, 26% of the available volume is empty; the interstitial space permits the insertion or intercalation of metal ions between the C_{60} molecules, as shown in figure 1. In contrast to the two-dimensional graphite intercalation compounds, solid C_{60} is a three-dimensional material that has two tetrahedral sites and one octahedral site per C_{60} molecule. Thus the intercalated solid has the stoichiometry A_3C_{60} when each of the available sites is filled with a single atom A. (See the middle panel of figure 1.)

In studying these new materials, my colleagues at AT&T Bell Laboratories and I found that the intercalation of alkali metal atoms into these interstitial sites gives rise to metallic behavior in an otherwise insulating solid.[4] Testing for superconductivity, we found[5] that potassium-doped C_{60} has a superconducting transition at a surprisingly high temperature—greater than 18 K. (In comparison, the related graphite intercalation compound KC_8, in which the potassium atoms are sandwiched between the graphite planes, has a transition temperature of only a few tenths of a kelvin.) In this initial work, we unequivocally demonstrated superconductivity in thin films when we observed transitions to zero resistance. Microwave loss and magnetization measurements revealed superconductivity in bulk powders. Progress sometimes comes by leaps and bounds, and in this case our group[6] and a group at the University of California at Los Angeles[7] found that doping with rubidium produced a material with a transition temperature—a sizzling 29 K—more than 50% higher than that of the potassium-doped compound. The potassium-doped C_{60} has the stoichiometry[7] K_3C_{60}, and its structure, determined by x-ray diffraction, is face-centered cubic.[8]

This work created quite a commotion, for here was a new class of materials involving only two elements—carbon and an alkali metal—that appeared to be a contender, along with the cuprates, for record high transition temperatures. Although the T_c's of the new carbon-based superconductors now appear to have peaked in the mid-30-kelvin range, interest and speculation have not subsided. There are still open scientific questions about the mechanism that gives rise to such unexpectedly high transition temperatures, and there is a feeling that the lessons learned in studying alkali-metal-doped C_{60}

Arthur Hebard is a member of the technical staff at AT&T Bell Laboratories in Murray Hill, New Jersey.

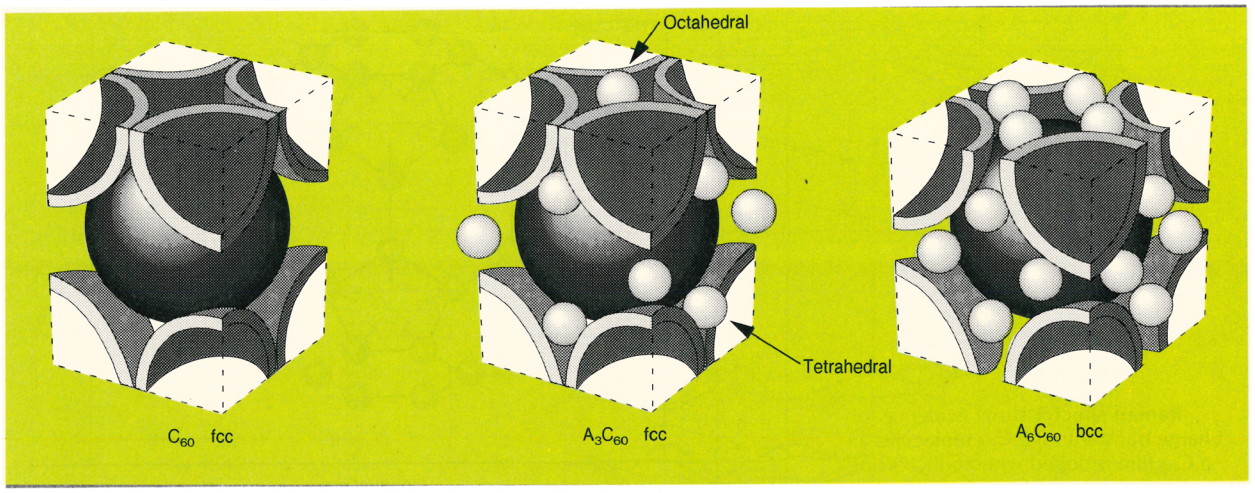

Structures of pristine and alkali-metal-doped C_{60}. The structure of solid C_{60} is a face-centered-cubic cell (shown in the body-centered-tetragonal representation in the left panel). There are three interstitial sites available per C_{60} unit for intercalated alkali metal atoms A (center): Two of the sites provide tetrahedral coordination (four nearest C_{60} neighbors), and one allows octahedral coordination (six nearest neighbors). For stoichiometries greater than three A atoms per C_{60}, the crystal expands and transforms to different structures: a bct structure (not shown) for A_4C_{60} and a body-centered-cubic structure (right panel) for A_6C_{60}. (Adapted from ref. 8.) **Figure 1**

might well lead to new approaches in the design of organic molecular materials having much improved superconducting properties.

From insulator to conductor to insulator

Our group at Bell Labs first observed electrical conductivity in doped C_{60} films by mounting electrically insulating C_{60} films in evacuated glass tubes and then exposing the films to alkali metal vapor.[4] As the exposure increased, the films changed color from the pristine yellow characteristic of vapor-sublimed films to the grayish hue of a typical metallic film. Simultaneously, we measured electrical properties and found that for each of the alkali metals (Li, Na, K, Rb and Cs) the resistivity decreased with exposure time, reached a minimum and then increased again toward the insulating state. The lowest resistivity (approximately 2 mΩ cm) was obtained with the potassium-doped compound, identifying it as the candidate most likely to exhibit superconducting behavior.

The high electron affinity of the C_{60} molecule[9] and the low ionization potentials of alkali metals suggest that the alkali-metal-doped fullerenes are ionic compounds in which electrons are completely transferred to the neutral C_{60} molecules. We have demonstrated this electron transfer using Raman scattering to monitor the shift in frequency of the $A_g(2)$ vibrational mode during doping.[4] (See figure 2.) For the $A_g(2)$ mode the atomic motions lie predominantly in the planes of the pentagons and the hexagons: The pentagonal ring "breathes" in and out symmetrically, while the bonds around the hexagons alternately expand and contract. The $A_g(2)$ pentagonal breathing mode shifts to lower frequency as the doping exposure—and the amount of charge transferred—increases. The interesting feature of the data in figure 2 is that the $A_g(2)$ vibrational frequency continues to shift even as the C_{60} film is doped beyond the resistance minimum. With further doping the insulating state again occurs, and the $A_g(2)$ frequency saturates at a frequency shifted by an amount equal to the frequency shift between the pristine and maximally conducting films. Additional alkali metal vapor is not absorbed by the saturated insulating phase but rather segregates out as pure alkali metal on the surface of the doped film.

Central to an understanding of conductivity in crystalline solids is knowledge of the electronic structure. The C_{60} molecule can be thought of as a "spherical porcupine" in which 60 electrons occupy π orbitals that have mostly p-like character and project radially from the surface of the molecule. Hückel calculations[9] for the isolated C_{60} molecule (see the left-hand portion of figure 3) show the relative positioning in energy of these molecular orbitals. The π electrons pair up to fill 30 energy states. The degeneracy of the angular momentum $L = 5$ level, which contains 11 states, is removed by the icosahedral symmetry of the molecule, resulting in three separate levels: the h_u, or highest occupied molecular orbital (HOMO), containing 10 electrons; the triply degenerate t_{1u} lowest unoccupied molecular orbital (LUMO), which can accommodate 6 electrons; and a similar triply degenerate t_{2u} orbital (the LUMO + 1) at higher energy.

The explanation, then, for the change in conductivity with doping is that the t_{1u} LUMO fills with electrons in proportion to the number of intercalated A atoms. Thus for a symmetric band at half filling (three electrons in the band), the density of states is maximum and the conductivity is also maximum. However, when the band is completely filled, with six electrons, there are no empty states into which the electrons can scatter, and the material becomes an insulator again, as it was when the band was empty. To accommodate additional A atoms, the fcc structure with a half-filled band and stoichiometry A_3C_{60} transforms to a more open structure (see the right-hand panel of figure 1), which has been identified in crystalline powder samples by x-ray diffraction[8] to be body-centered cubic. Experimenters have also identified[9] a body-centered tetragonal phase with stoichiometry A_4C_{60}, where A can be potassium, rubidium or cesium. Thus attempts to fill the conduction band of A_xC_{60} beyond half filling ($x = 3$) result in insulating bct and bcc phases

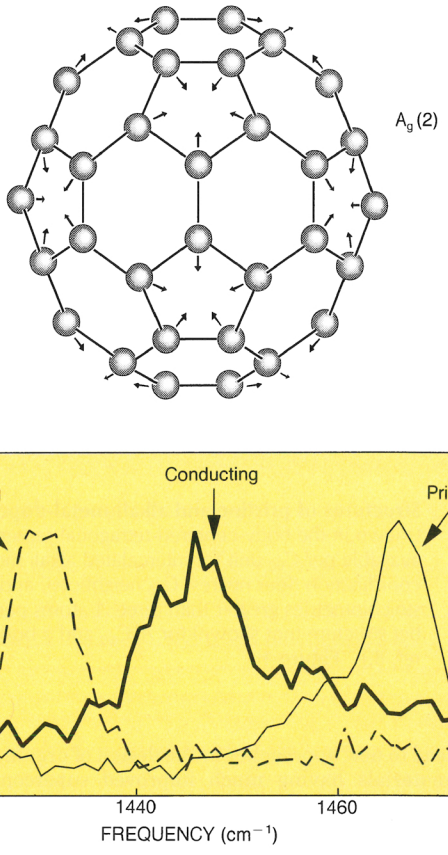

Raman spectra show evidence for charge transfer to the C_{60} molecules as a C_{60} film is doped with an increasing number of potassium atoms. Among the ten allowed Raman-active vibrational modes, the $A_g(2)$ pentagonal breathing mode (depicted at top) has a particularly high cross section. As the proportion of dopant increases, electrons are added to the antibonding orbitals, and the molecule oscillates at a lower frequency. The amount of charge necessary to convert the pristine, insulating C_{60} to the maximally conducting phase is three electrons per C_{60}. Adding three more electrons per C_{60} transforms the conducting solid to the filled-band insulating phase. (Adapted from ref. 4.) **Figure 2**

that can incorporate, respectively, four and six A atoms per C_{60}.

Band structure calculations,[10] the results of which are shown in figure 3 for the metallic solid K_3C_{60}, reveal important details. Despite the spaghetti-like band dispersion that describes the dependence of the electron energy on wavevector within each band, the correspondence of the bands in the solid to the orbitals of the isolated molecule is immediately evident. The energy of the potassium 4s orbitals is high enough that it undergoes no strong hybridization, or mixing, with the C_{60} LUMO. An important consequence of the transfer of electrons from the K 4s orbitals to the t_{1u}-derived orbitals of the pristine C_{60} solid is that the material becomes not only metallic but also highly ionic, with a large cohesive energy. The ionized potassium atoms act like an electrostatic glue holding the otherwise weakly bound C_{60} molecules together and, after donating their 4s electrons, play no major role in the electronic properties of the solid. Thus the molecular framework of the pristine solid provides the electronic pathways to accommodate the donated electrons in extended states. And these extended states provide the basis for the metallic and superconducting properties of the A_3C_{60} compounds.

Phenomenology of superconductivity

Experimenters at various laboratories are now turning considerable attention toward exploring the phenomenology of superconductivity in doped fullerenes. Current efforts to study films, crystals and powders have been somewhat frustrated, however, by the extreme air sensitivity of these compounds. In the presence of air, the reduced C_{60} molecules readily return their extra electrons to their donors, which form alkali metal oxides or hydroxides that precipitate on the crystallite surfaces or in grain boundaries between crystallites. Raman scattering results that show the frequency of the $A_g(2)$ mode shifting back to its value in the pristine compound when the sample is exposed to air demonstrate that the C_{60} reversibly returns to its original charge state. This extreme sensitivity to oxidation requires the preparation of samples in an inert environment and experimentation on *in situ*-prepared or encapsulated samples. In addition, one must assure stoichiometric control and anneal samples at temperatures high enough (at least 250 °C) to guarantee uniform dispersal of the alkali intercalants. [The precision to which x in K_xC_{60} has been measured ($x = 3.00 \pm 0.05$) for a variety of film thicknesses[11] indicates that the superconducting phase occurs exactly at half band filling.] Despite these difficulties, researchers have pieced together a reasonably coherent picture of the superconducting properties of these alkali-metal-doped fullerenes.

One of the clues to understanding the superconductivity comes from the dependence of the superconducting transition temperatures T_c of the A_3C_{60} or $A_{3-x}A'_xC_{60}$ compositions on lattice parameter.[12] As figure 4 shows, the larger intercalant ions cause lattice expansion and a corresponding increase in T_c. Similarly, increasing the pressure on a sample reduces the lattice spacing and concomitantly the T_c. Knowing the compressibility, one can convert the pressure dependence to a dependence on lattice constant[13] and plot it, as is done in figure 4 for K_3C_{60} and Rb_3C_{60}. That one can apply pressure to reduce the lattice constant and the T_c of Rb_3C_{60} to the same values as in unpressurized K_3C_{60} implies that it is the electronic

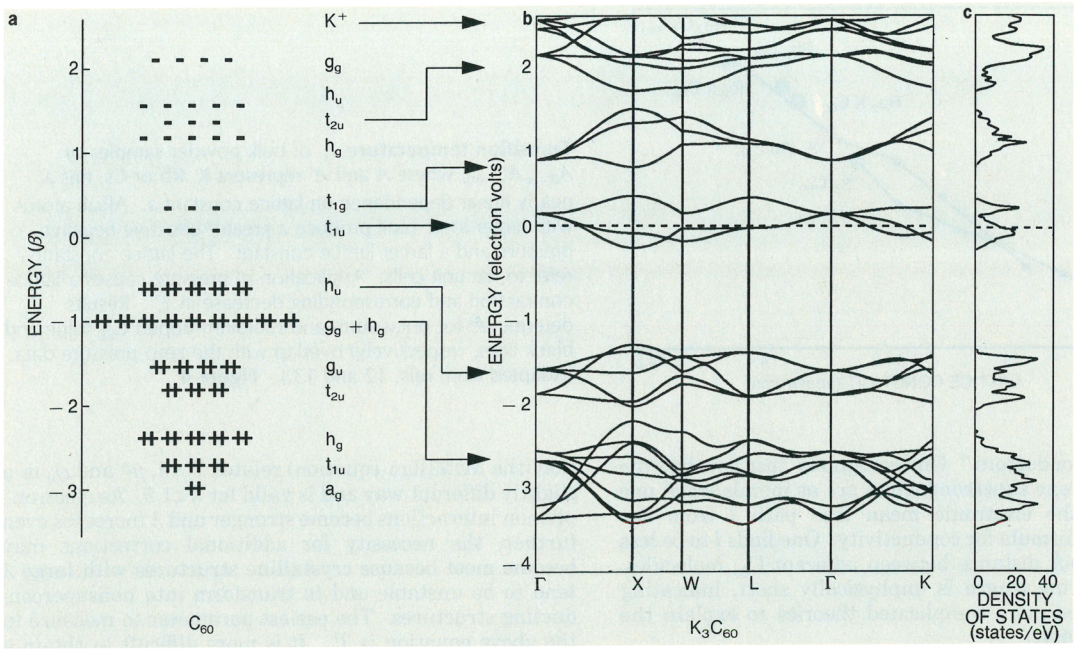

Results of electronic energy calculations demonstrate how the molecular character of the energy states of the isolated C_{60} molecule is preserved in the energy band structure of the metallic K_3C_{60} compound. **a**: Hückel calculations reveal the symmetry, degeneracy and occupancy of the energy levels of the neutral C_{60} molecule. The labels a, t, g and h refer to degeneracies of 1, 2, 4 and 5, respectively; the subscripts g and u refer respectively to even (*gerade*) and odd (*ungerade*) symmetry. The proximity of the t_{1u} lowest unoccupied molecular orbital to the zero of the Hückel energy axis indicates that the isolated molecule has a high electron affinity. **b**: Local density approximation calculations for K_3C_{60} show the dependence of electronic energy on wavevector. Each band can be matched with its counterpart in the isolated molecule. The Fermi energy (dashed line) intersects two of the t_{1u} bands and occupies a position close to one of the peaks in the density of states (**c**). (Adapted from refs. 9 and 10.) **Figure 3**

overlap between wavefunctions on the C_{60} molecules and not the type of alkali metal atom that is important for superconductivity. Attempts to expand the lattice further with larger ions and obtain T_c's beyond the maximum of 33 K reported[12] for the composition $RbCs_2C_{60}$ will be frustrated by structural transformations driven by charge or magnetic instabilities that would become enhanced as the band overlap between nearest neighbors decreased.

It is difficult to understand the electronic properties of the doped C_{60} superconductors without realizing that the doped material comprises immiscible and stoichiometrically distinct phases. The number of distinct phases is small; for A_xC_{60} (where A is K or Rb) only pristine C_{60}, conducting A_3C_{60} and insulating A_4C_{60} and A_6C_{60} phases have been identified by x-ray diffraction. There are no indications of other phases. Thus in the vapor-phase doping of K_xC_{60}, for example, K_3C_{60} nucleates and grows as islands surrounded by insulating C_{60}. At $x = 3$ the islands coalesce as all of the C_{60} is converted to K_3C_{60}. This scenario for granular growth in which only the pure C_{60} and K_3C_{60} phases are observed has also been confirmed by ^{13}C nuclear magnetic resonance.[14] At $x = 0$ the nmr spectrum reveals only a single motionally narrowed line, because all the carbon atoms are equivalent and the effective magnetic field seen by each atom is averaged by the rapid room temperature rotation of the molecules. As doping proceeds, this line diminishes in intensity and another single line at higher frequency, associated with K_3C_{60}, increases in intensity, until at maximum conductivity the second line is the only one present. If the global stoichiometry is not precisely at 3, then there are insulating phases present (C_{60} for $x < 3$ and K_4C_{60} or K_6C_{60} for $x > 3$) that, by acting as barriers to electronic conduction between grains, degrade the conducting properties of the material and lead to a diminished ability to sustain large supercurrents.[11]

Granular microstructure can have a profound effect on superconducting properties.[15] The temperature at which the resistance vanishes in granular K_3C_{60} films is near 12 K (compared with greater than 19 K in bulk material), with most of the resistance drop occurring over an interval of 1 K. One can attribute this reduced T_c to Coulomb charging effects, which become particularly important when the grains are small (60 Å in diameter, as determined by x-ray diffraction). Also, analysis of the temperature dependence of the excess conductivity above T_c shows the importance of zero-dimensional fluctuations, which typically occur when small superconducting grains are weakly coupled. In contrast, doped crystals have, in addition to a higher T_c, a temperature dependence typical of a metal above T_c and a sharper transition without any evidence of zero-dimensional fluctuations.[16] Although much of this difference can be attributed to grain size, it is interesting that the room temperature resistivities ρ_n (2.5 mΩ cm) for the films are a factor of 2 lower than those of the best crystals reported to date. Thus the question of what value to attribute to the intrinsic normal-state resistivity is somewhat undecided. The measured values are rather high for a typical metal, giving credence to the impression that "bad metals with high resistivity make

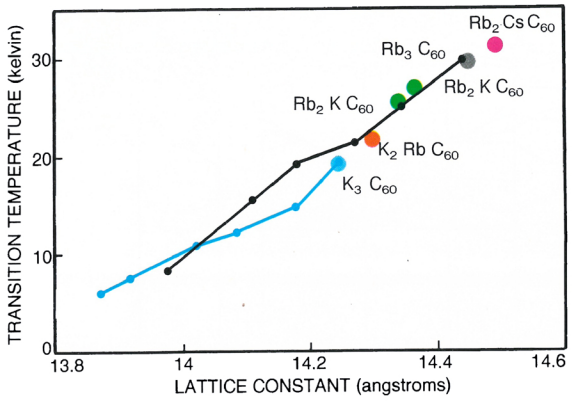

Transition temperature T_c of bulk powder samples of $A_{3-x}A'_xC_{60}$, where A and A' represent K, Rb or Cs, has a nearly linear dependence on lattice constant a. Alkali atoms with larger ionic radii produce a greater effective negative pressure and a larger lattice constant. The lattice constants refer to fcc unit cells. Application of pressure causes a lattice contraction and corresponding decrease in T_c. Results determined for potassium- and rubidium-doped C_{60} (blue and black lines, respectively) overlap with the zero-pressure data. (Adapted from refs. 12 and 13.) **Figure 4**

good superconductors." One recognizes just how bad the doped fullerene superconductors are as metals when one calculates the electronic mean free path l from the Boltzmann formula for conductivity. One finds l to be less than the 10-Å distance between adjacent C_{60} molecules. This scattering length is unphysically short, indicating that we need more complicated theories to explain the high resistivity.

Two important temperature-dependent characteristic lengths, the coherence length ξ and the penetration length λ_p, are associated with the magnetic properties of a superconductor. The coherence length ξ is a measure of the spatial extent of a superconducting pair and defines the minimum distance over which superconductivity can be quenched. One can calculate ξ from the expression $2\pi H_{c2}(T)\,\xi(T)^2 = \Phi_0$, where Φ_0 is the flux quantum and H_{c2} is the upper critical field, which delineates the phase boundary between superconducting and normal states. This field can be determined from resistance transitions in different magnetic fields[15] or by magnetization measurements.[17] Both techniques give a value of H_{c2} for K_3C_{60} that extrapolates to a zero-temperature ($T = 0$) value on the order of 50 tesla (measured to be closer to 30 T) and yields a calculated $\xi(0)$ of 26 Å. That small value is comparable to the values measured for the high-T_c cuprates and much smaller than, say, the 400-Å value for niobium. The penetration length λ_p is inversely proportional to the density of superconducting pairs (and thus the electron density) and defines the distance over which a magnetic field will penetrate into a superconductor. It has been measured by magnetization[17] and muon-spin relaxation[18] techniques and has a value for K_3C_{60} between 2400 and 4800 Å. Accordingly, doped fullerene superconductors are of extreme type II ($\lambda_p/\xi \gg 1$) and reside somewhere between the clean ($l \gg \xi$) and dirty ($l \ll \xi$) limits.

Mechanisms for pairing

Superconductivity is a highly correlated many-body state of a metal. The transition temperature T_c is well described by the Bardeen–Cooper–Schrieffer equation,

$$T_c = \omega_0 e^{-1/(\lambda - \mu^*)}$$

in the weak-coupling limit ($\lambda \ll 1$), where the parameter λ is the product of the density of states at the Fermi energy $N(E_F)$ and a coupling matrix V, which is a measure of the strength of the interaction between electrons and excitations (usually phonons) having a characteristic frequency ω_0. The coupling represented by λ is reponsible for the pairing interaction and, for superconductivity to occur, needs to be larger than the μ^* term describing the electron–electron repulsion. A strong-coupling T_c equation (the McMillan equation) relates T_c, λ, μ^* and ω_0 in a slightly different way and is valid for $\lambda \leqslant 1.5$. As electron–phonon interactions become stronger and λ increases even further, the necessity for additional corrections may become moot because crystalline structures with large λ tend to be unstable and to transform into nonsuperconducting structures. The easiest parameter to measure in the above equation is T_c. It is more difficult to obtain a consensus for the other parameters, and at best the range of theoretical interpretations is constrained by an envelope of measured or inferred values.

Theories describing superconductivity in alkali-metal-doped fullerenes can be placed in two categories: those in which the electron–phonon coupling is important and those in which the electron–electron interactions are important.[19] If electron–phonon coupling is responsible for the superconductivity, then it is necessary to take a close look at the relative importance of different vibrational modes. Figure 5 shows the spectrum of vibrations in the doped fullerene compounds and hence delineates the possible vibrational frequencies ω_0 that may be important to electron–phonon coupling. In order of increasing frequency, there are the librational (rocking) motions of individual C_{60} molecules, followed by the intermolecular modes, in which C_{60} molecules vibrate with respect to their neighbors; the optic modes, in which C_{60} molecules are coupled to their ionized metal donors; and the intramolecular, or "on ball," modes. The intramolecular modes tend to have a more radial character at low frequencies and a more tangential character at high frequencies, as illustrated in figure 5 by the $H_g(1)$ and $H_g(7)$ modes. The theories explaining superconductivity with an electron–phonon mechanism[20] give varying weights to these modes, the general trend being that if the low-frequency modes are important, then λ must be large, and vice versa. Thus one model, which emphasizes the lower-frequency intramolecular modes with an average frequency near 350 cm^{-1}, would require $\lambda = 1$; a second model, which includes contributions from a broad range of H_g modes with an average frequency near 900 cm^{-1}, would require $\lambda = 0.6$; and a third one, which calculates significant coupling only to the two highest H_g modes near 1500 cm^{-1}, would require $\lambda = 0.5$.

Researchers have compared the relative vibrational frequencies (from Raman and inelastic neutron scattering spectra) of pristine C_{60} and K_3C_{60} to infer the extent of electron coupling to identifiable vibrations.[20] The most direct evidence for phonon-mediated pairing, however, comes from isotope-effect measurements[21] in which the T_c of 100% ^{13}C-substituted K_3C_{60} (black dots in figure 6) is compared with the T_c of unsubstituted K_3C_{60} (blue dots). If only the intramolecular, or on-ball, modes are important

for superconductivity, so that $\omega_0 \propto M^{-1/2}$ (where M is the mass of the C_{60} molecule), then $\delta T_c = -\frac{1}{2}(\delta M/M)T_c$ is calculated to be -0.8 K, a factor of 2 greater difference than is observed. The discrepancy is attributed to strong-coupling corrections and inclusion of the M dependence in the μ^* term.[21] Interestingly, one can also explain the 0.4-K decrease in T_c for $K_3{}^{13}C_{60}$ by assuming that the pairing interaction giving rise to superconductivity is not mediated by phonons but is purely electronic in origin.[19]

For intramolecular vibrational modes, the electron–phonon coupling energy V, an on-ball quantity, is independent of lattice constant a, and the dependence of $\lambda = N(E_F)V$ on a can be subsumed into $N(E_F)$. Thus the dependence of T_c on a (shown in figure 4) can, within the BCS electron–phonon model, be attributed to the dependence of $N(E_F)$ on a. Simply stated, as the lattice expands, the electronic overlap between adjacent molecules decreases, and the reduced bandwidth leads to a larger $N(E_F)$ and, according to the BCS equation, an increased T_c. One reaches a similar conclusion with the all-electronic superconductivity mechanism mentioned above.[19] Estimates of $N(E_F)$ for both K_3C_{60} and Rb_3C_{60} have been obtained from magnetization measurements of the normal-state susceptibility and nmr measurements of the ^{13}C spin relaxation time.[22] The results from these separate experiments—densities of states of 28–35 states/eV-C_{60} for potassium and 38–44 states/eV-C_{60} for rubidium—allow a calibration of the slope of T_c (shown in figure 4) with respect to a change in density of states. Roughly, the 60% higher T_c of Rb_3C_{60} compared to K_3C_{60} correlates with a 30% increase in $N(E_F)$. Furthermore, the inferred bandwidth $W_{t_{1u}}$ for the six allowed states in the t_{1u} conduction band of the potassium compound can be approximated as $W_{t_{1u}} = 6/N(E_F) \sim 0.2$ eV. This value is a factor of 3 less than the band structure result[10] displayed in figure 3. Such narrow bandwidths and correspondingly low Fermi energies ($E_F = W_{t_{1u}}/2 \sim 0.1$ eV) are characteristic of molecular solids in which the orbital overlap between adjacent clusters is small.

With the experimental results now in hand, it is easy to adopt the view that high-T_c superconductivity in the alkali-metal-doped fullerenes can be explained by a conventional (BCS) electron–phonon mechanism. There are serious problems with this viewpoint, however, because the parameters of the theory have been pushed to the limit of applicability. For example, because ω_0 and E_F are approximately equal, with values in the range of a few tenths of a volt, the usual approximation $\omega_0 \ll E_F$ no longer holds. In addition, Coulomb repulsion energies may be comparable to the conduction bandwidth, making A_3C_{60} perilously close to becoming an insulator. Furthermore, disorder in the orientations of the molecules may provide additional scattering and, concomitantly, extremely short mean free paths. And little is understood theoretically or experimentally about electron–electron correlations as represented in the parameter μ^*. Narrow electronic bands with enhanced Coulomb repulsions are not favorable for the formation of superconducting paired electrons. If, however, the electrons can make transitions to higher energy states and escape to neighboring C_{60} molecules before becoming correlated with each other, then this repulsion effect is considerably lessened. If not, then we may need to invoke pairing mechanisms[19] other than electron–phonon.

Superconductivity in doped fullerenes presents an exciting challenge to physicists, chemists and materials scientists. Already, superconductivity has been demonstrated with a $T_c = 8.4$ K with the divalent group IIA intercalant calcium,[23] and one can glean numerous alternative combinations from the periodic table. At present the mechanism for high T_c is not agreed upon, physical characterization is not complete, and the high

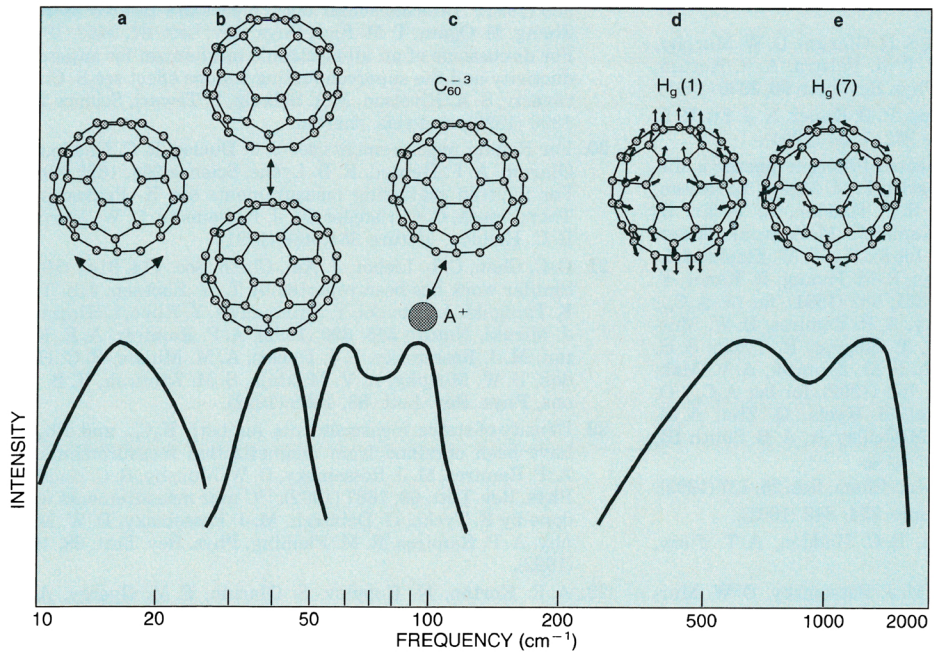

Various vibrations in the A_3C_{60} compounds can contribute to electron–phonon coupling and may be important for superconductivity. At lower energies the compounds exhibit librational modes of individual C_{60} molecules (**a**), intermolecular modes (**b**) and optic modes (**c**). At higher energies the intramolecular modes dominate; these "on ball" modes have a radial character (**d**) at lesser energies (for example, the $H_g(1)$ mode) and a tangential character (**e**) at greater energies (for example, the $H_g(7)$ mode). (Depiction of on-ball modes courtesy of M. Grabow and K. Raghavachari, AT&T Bell Labs.) **Figure 5**

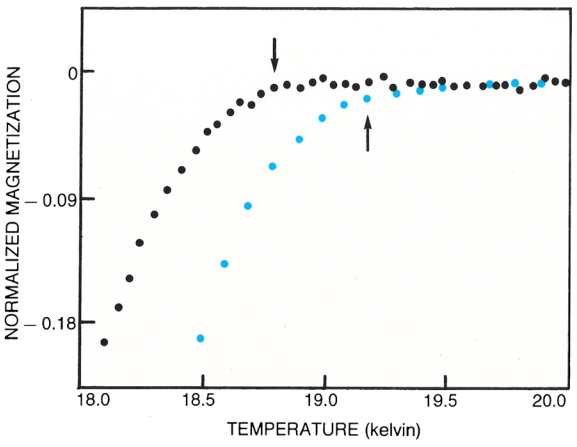

Magnetization transition in isotopically pure $K_3{}^{13}C_{60}$ (black) occurs at a temperature 0.4 K lower than in $K_3{}^{12}C_{60}$ (blue). Transition temperatures are marked by arrows. The samples were initially cooled to 5 K in zero field, and the magnetization was measured on warming in a 20-oersted field. (Adapted from ref. 21.) **Figure 6**

reactivity of the doped phases is a daunting obstacle to practical applications. Nevertheless, the discovery that a new class of three-dimensional molecular solids can be transformed by intercalation into conducting and superconducting compounds is expected to initiate further advances, with consequences currently unforeseen.

* * *

I gratefully acknowledge the invaluable collaborations and stimulating discussions I have had with colleagues at AT&T Bell Laboratories and elsewhere.

References

1. H. W. Kroto, J. R. Heath, S. C. O'Brien, R. F. Curl, R. E. Smalley, Nature **318**, 162 (1986).
2. W. Krätschmer, L. D. Lamb, K. Fostiropoulos, D. R. Huffman, Nature **347**, 354 (1990).
3. For a review, see M. S. Dresselhaus, G. Dresselhaus, Adv. Phys. **30**, 139 (1981).
4. R. C. Haddon, A. F. Hebard, M. J. Rosseinsky, D. W. Murphy, S. J. Duclos, K. B. Lyons, B. Miller, J. M. Rosamilla, R. M. Fleming, A. R. Kortan, S. H. Glarum, A. V. Makhija, A. J. Muller, R. H. Eick, S. M. Zahurak, R. Tycko, G. Dabbagh, F. A. Thiel, Nature **350**, 320 (1991).
5. A. F. Hebard, M. J. Rosseinsky, R. C. Haddon, D. W. Murphy, S. H. Glarum, T. T. M. Palstra, A. P. Ramirez, A. R. Kortan, Nature **350**, 600 (1991).
6. M. J. Rosseinsky, A. P. Ramirez, S. H. Glarum, D. W. Murphy, R. C. Haddon, A. F. Hebard, T. T. M. Palstra, A. R. Kortan, S. M. Zahurak, A. V. Makhija, Phys. Rev. Lett. **66**, 2830 (1991).
7. K. Holczer, O. Klein, S.-M. Huang, R. B. Kaner, K.-J. Fu, R. L. Whetten, F. Diederich, Science **252**, 1154 (1991).
8. X-ray identification of the indicated fullerene phases is discussed by R. M. Fleming, T. Siegrist, P. M. Marsh, B. Hessen, A. R. Kortan, D. W. Murphy, R. C. Haddon, R. Tycko, G. Dabbagh, A. M. Mujsce, M. L. Kaplan, S. M. Zahurak, Mater. Res. Soc. Symp. **206**, 691 (1991), for fcc C_{60}; P. W. Stephens, L. Mihaly, P. L. Lee, R. L. Whetten, S.-M. Huang, R. Kaner, F. Diederich, K. Holczer, Nature **351**, 632 (1991), for fcc A_3C_{60}; R. M. Fleming, M. J. Rosseinsky, A. P. Ramirez, D. W. Murphy, J. C. Tully, R. C. Haddon, T. Siegrist, R. Tycko, S. H. Glarum, P. Marsh, G. Dabbagh, S. M. Zahurak, A. V. Makhija, C. Hampton, Nature **352**, 701 (1992), for bct A_4C_{60}; O. Zhou, J. E. Fischer, N. Coustel, S. Kycia, Q. Zhu, A. M. McGhie, W. J. Romanow, J. P. McCauley Jr, A. B. Smith III, Nature **351**, 462 (1991), for bcc A_6C_{60}.
9. For a review, see R. C. Haddon, Acc. Chem. Res. **25**, 127 (1992).
10. S. C. Erwin, W. E. Pickett, Science **254**, 842 (1991).
11. G. P. Kochanski, A. F. Hebard, R. C. Haddon, A. T. Fiory, Science **255**, 184 (1992).
12. R. M. Fleming, A. P. Ramirez, M. J. Rosseinsky, D. W. Murphy, R. C. Haddon, S. M. Zahurak, A. V. Makhija, Nature **352**, 787 (1991). The maximum T_c of 33 K in this series was reported by K. Tanigawa, T. W. Ebbesen, S. Saito, J. Mizuki, J. S. Tsai, Y. Kubo, S. Kuroshima, Nature **352**, 222 (1991).
13. See O. Zhou, G. B. M. Vaughan, Q. Zhu, J. E. Fischer, P. A. Heiney, N. Coustel, J. P. McCauley, A. B. Smith, Science **255**, 833 (1992), and refs. therein.
14. R. Tycko, G. Dabbagh, M. J. Rosseinsky, D. W. Murphy, R. M. Fleming, A. P. Ramirez, J. C. Tully, Science **353**, 884 (1991).
15. T. T. M. Palstra, R. C. Haddon, A. F. Hebard, J. Zaanen, Phys. Rev. Lett. **68**, 1054 (1992).
16. X.-D. Xiang, J. G. Hou, G. Breceño, W. A. Bareka, R. Mostovoy, A. Zettl, V. H. Crespi, M. L. Cohen, Science **256**, 1190 (1992).
17. K. Holczer, O. Klein, G. Grüner, J. D. Thompson, F. Diederich, R. L. Whetten, Phys. Rev. Lett. **67**, 271 (1991). G. Sparn, J. D. Thompson, R. L. Whetten, S.-M. Huang, R. B. Kaner, F. Diederich, G. Grüner, K. Holczer, Phys. Rev. Lett. **68**, 1228 (1992).
18. Y. J. Uemura, A. Keren, L. P. Lee, G. M. Luke, B. J. Sternlieb, W. D. Wu, J. H. Brewer, R. L. Whetten, S.-M. Huang, S. Lin, R. B. Kaner, F. Diederich, S. Donovan, G. Grüner, K. Holczer, Nature **352**, 605 (1991).
19. Theoretical papers that treat electron–phonon coupling for intramolecular modes include R. A. Jishi, M. S. Dresselhaus, Phys. Rev. B **45**, 2597 (1992); M. Schluter, M. Lanoo, M. Needles, G. A. Baraff, D. Tomanek, Phys. Rev. Lett. **68**, 526 (1991); C. M. Varma, J. Zaanen, K. Raghavachari, Science **254**, 989 (1991). Intermolecular optic modes are treated by F. C. Zhang, M. Ogata, T. M. Rice, Phys. Rev. Lett. **67**, 3452 (1991). For discussions of an all-electronic mechanism for superconductivity and the superconducting isotope effect see S. Chakravarty, S. A. Kivelson, M. I. Salkola, S. Tewari, Science **256**, 1306 (1992), and refs. therein.
20. For Raman measurements see S. J. Duclos, R. C. Haddon, S. Glarum, A. F. Hebard, K. B. Lyons, Science **254**, 1625 (1991). For neutron scattering measurements see K. Prassides, J. Thomkinson, C. Christedes, M. J. Rosseinsky, D. W. Murphy, R. C. Haddon, Nature **354**, 462 (1991).
21. C.-C. Chen, C. L. Lieber, J. Am. Chem. Soc. **114**, 3141 (1992). Similar work has been reported by T. W. Ebbesen, J. S. Tsai, K. Tanigaki, J. Tabuchi, Y. Shimakawa, Y. Kubo, I. Hirosawa, J. Mizuki, Nature **355**, 620 (1992); A. P. Ramirez, A. R. Kortan, M. J. Rosseinsky, S. J. Duclos, A. M. Mujsce, R. C. Haddon, D. W. Murphy, A. V. Makhija, S. M. Zahurak, K. B. Lyons, Phys. Rev. Lett. **68**, 1058 (1992).
22. Density-of-states measurements for both K_3C_{60} and Rb_3C_{60} have been obtained from magnetization measurements by A. P. Ramirez, M. J. Rosseinsky, D. W. Murphy, R. C. Haddon, Phys. Rev. Lett. **69**, 1687 (1982); ^{13}C nmr measurements were done by R. Tycko, G. Dabbagh, M. J. Rosseinsky, D. W. Murphy, A. P. Ramirez, R. M. Fleming, Phys. Rev. Lett. **68**, 1912 (1992).
23. A. R. Kortan, N. Kopylov, S. Glarum, E. M. Gyorgy, A. P. Ramirez, R. M. Fleming, F. A. Thiel, R. C. Haddon, Nature **355**, 529 (1992). ■